Journal of Structural Geology, Vol. 12, No. 7, pp. 805 to 821, 1990
Printed in Great Britain

0191-8141/90 $03.00 + 0.00

Structural characteristics of granitic plutons emplaced during weak regional deformation: examples from late Carboniferous plutons, Morocco

JEAN LOUIS LAGARDE

Laboratoire de Tectonophysique, CAESS, 35042 Rennes Cédex, France

SAAD AIT OMAR

Departement de Géologie, Faculté des Sciences, BP S 15, Marrakech, Maroc

and

BERNARD RODDAZ

Laboratoire de Géologie, Faculté des Sciences, 64000 Pau, France

(*Received* 21 *March* 1989; *accepted in revised form* 6 *February* 1990)

Abstract—Strain patterns have been investigated around shallow crustal granitic plutons emplaced during weak regional deformation in the Western Moroccan Hercynian belt. The plutons are distributed along reactivated deep faults and display elliptical shapes which are consistently oriented with respect to the regional strain field. Pluton age, orientation and ellipticity can be correlated with strain history. Ductile deformation and contact metamorphism are mainly located in the thermally softened aureoles. Finite strain gradients towards plutons are accompanied by the development of superimposed microstructures. Finite strain trajectories and variations of strain ellipsoid shapes exhibit perturbations of the regional strain field around plutons. Structures internal to the plutons are continuous with regional structures. Foliation development in granitoids records a decrease in temperature during syntectonic pluton cooling. Geometry and kinematics of deformation reflect the influence of both regional deformation and pluton intrusion.

INTRODUCTION

SHALLOW crustal plutons give rise to thermal softening (White & Knipe 1978, Brun & Cobbold 1980) in the surrounding aureoles and induce rheological heterogeneities in the crust. When the final emplacement of plutons interferes with regional deformation, thermal softening favours the concentration of deformation in the aureoles (Pitcher & Berger 1972, Sanderson & Meneilly 1981, Meneilly 1982, Bateman 1985). Strain patterns around such syntectonic plutons thus reflect both regional strain and intrusion effects (Brun & Pons 1981, Hutton 1982, Paterson & Tobisch 1988). These plutons ascend as diapiric tailed bubbles detached from their source (Ramberg 1970, Soula 1982, Hanmer & Vigneresse 1983) or assemble incrementally in their site of final emplacement by successive magma pulses (see review in Pitcher 1979). In some cases the final emplacement of plutons involves radial expansion or ballooning (Pitcher & Berger 1972, Brun & Pons 1981, Meneilly 1982, Bateman 1985).

This paper presents some characteristics of strain patterns around shallow crustal granitic plutons emplaced during a weak, low-grade deformation in the intracontinental Hercynian belt of Morocco (Fig. 1). Structural characteristics discussed are (1) distribution of plutons, (2) shape of plutons, (3) orientation of plutons with respect to the regional strain field, (4) distribution and microstructural evolution of the deformation in country rock, (5) strain intensity patterns, (6) variations of strain ellipsoid shapes, (7) finite strain trajectories, (8) syntectonic contact metamorphism and (9) foliation development and deformation mechanisms in granitoids.

LATE CARBONIFEROUS PLUTONS OF MOROCCO

Late Carboniferous plutons of Western Morocco were emplaced between 330 and 270 Ma (Tisserant 1977, Mrini 1985) and probably reflect post-collisional partial melting of the lower crust and upper mantle (Vogel *et al.* 1976, Mahmood & Bennani 1984, Mrini 1985). This process generated hot and dry crustal- and mantle-derived melts, able to intrude low-pressure regions of the upper crust (Cann 1970). The plutons studied involve three basic petrographic groups: I-type and mixed I–S-type biotite granodiorites (Termier & Termier 1971, Rosé 1987, Gasquet *et al.* 1988), S-type two mica monzogranites (Termier *et al.* 1950, Giuliani & Sonet 1982, Mahmood & Bennani 1984, Ait Omar 1986), and alkaline subsolvus granites emplaced during late Hercynian time (270 Ma) (Ait Ayad 1987, Mabkhout *et al.* 1988).

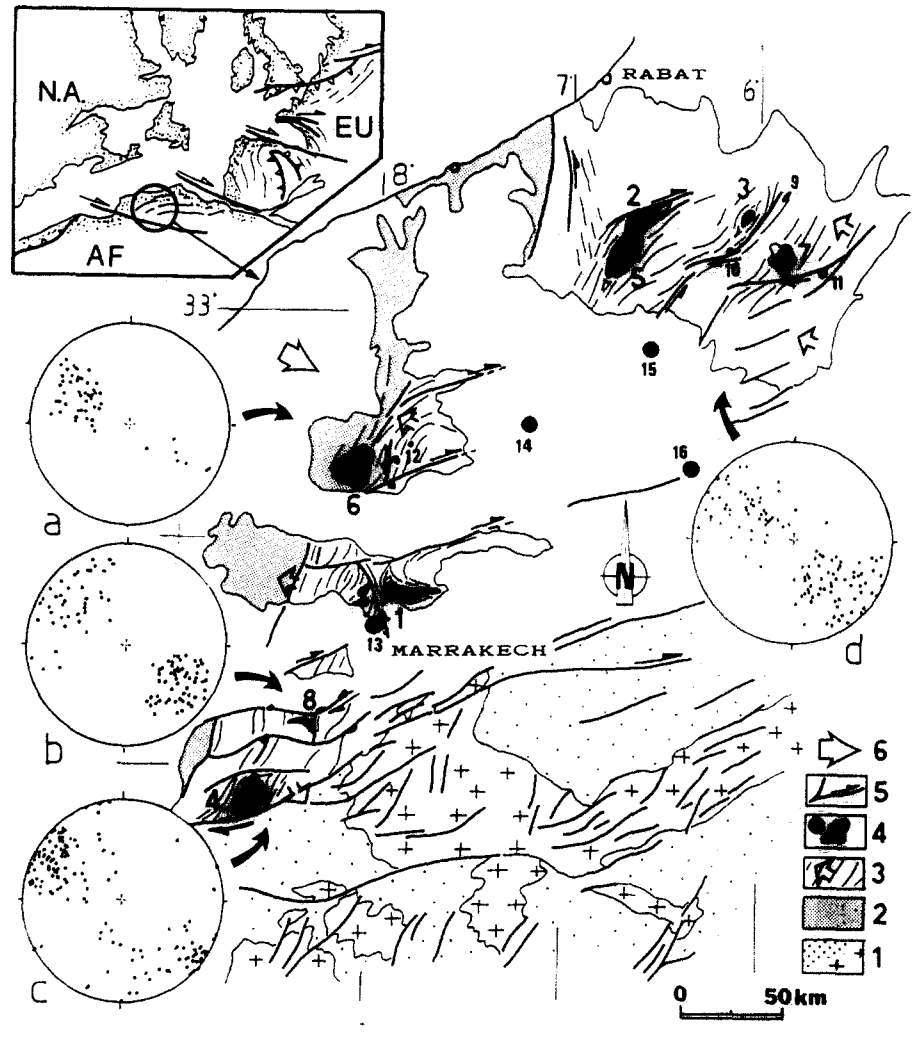

Fig. 1. Location of late Carboniferous plutons within the Western Moroccan Hercynian belt and adjacent areas. Inset: Western Morocco in the frame of the Hercynian orogeny (from Matte 1986). N.A.: North America. Af: Africa. Eu: Europe. 1: Proterozoic (crosses) and Paleozoic basement (dotted) in pre-Sahara foreland (from Choubert 1963). 2: Weakly deformed coastal block. 3: Western Moroccan Hercynian belt (from north to south: Central meseta, Rehamna, Jebilet, Occidental High Atlas), cleavage trajectories (thin lines) and general vergence (small open arrows). 4: Late Carboniferous plutons, from oldest to youngest, Jebilet granodiorite (1), Zaer granodiorite (2), Oulmes monzogranite (3), Tichka granitoids (4), Zaer monzogranite (5), Rehamna monzogranite (6), Ment granodiorite (7), Azegour monzogranites (8), smaller scale intrusions Achemeche, Mrirt, Moulay Bou Azza monzogranites (9–11), plutons recognized by geophysical (gravity) investigations (Van den Bosch 1974) (solid black circles) Marrakech, El Bourouj, Oued Zem, Beni Mellal plutons (13–16). 5: Basement fractures and late Carboniferous shear zones. 6: Direction of regional shortening. Stereonets: lower-hemisphere, equal-area projection of poles to regional schistosity. a: Rehamna, $n = 52$. b: Amizmiz–Ouirgane area, $n = 182$. c: Tichka $n = 144$. d: Zaer–Smalaa–Oulmes area $n = 122$.

Plutons were emplaced at shallow crustal Paleozoic levels (8–10 km depth) during the late Carboniferous deformation (Lagarde *et al.* 1989), the main Hercynian tectonic event in Western Morocco (Piqué & Michard 1989). This regional deformation is strongly heterogeneous. Narrow metamorphic and highly deformed zones (Lagarde & Michard 1986) contrast with larger weakly deformed areas with very low-grade metamorphism (Piqué 1982) (Fig. 2). In the deformed areas, foliation dips steeply, strikes NE–SW (Fig. 1) and contains a stretching lineation subparallel to the gently-plunging fold axes. Such a regional pattern is compatible with strike-slip motion related to ductile wrenching along pre-existing crustal fractures (Lagarde *et al.* 1989). Wrench faults occur in two sets with SSE sinistral and predominant ENE dextral displacements and display an asymmetric pattern suggesting a non-coaxial strain regime (Choukroune *et al.* 1987). The occurrence of zones containing a flat lying foliation and a down-dip stretching lineation indicates that thrusting is locally combined with the regional wrench faulting (Lagarde & Michard 1986).

PLUTON EMPLACEMENT AND REGIONAL DEFORMATION

In the Western Moroccan Hercynian belt, various features indicate that final emplacement of plutons was synchronous with late Carboniferous regional deformation.

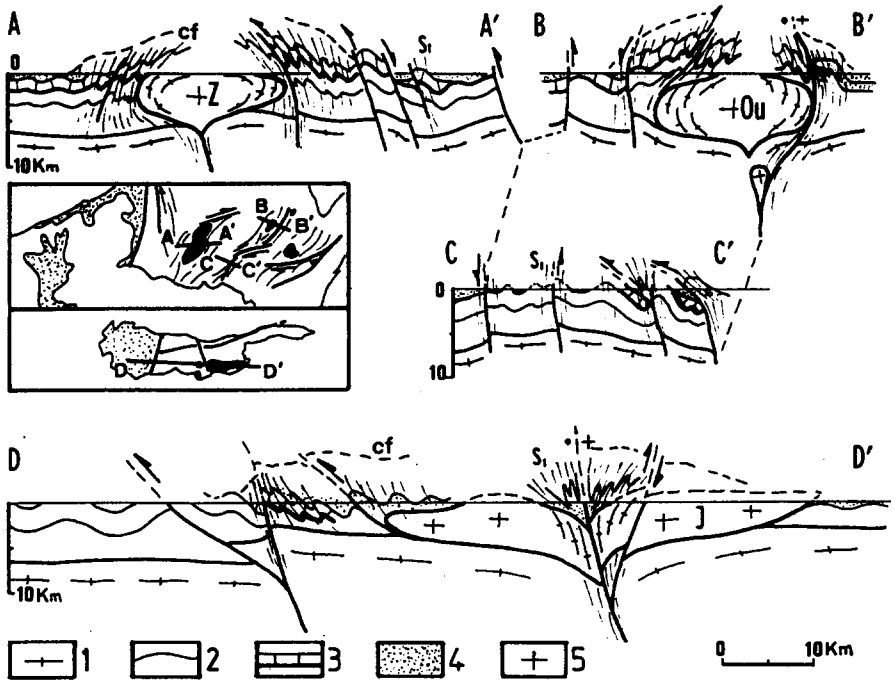

Fig. 2. Cross-sections illustrating heterogeneity of late Carboniferous deformation in Western Morocco. Ductile deformation mainly concentrates in zones of crustal weakness such as thermally softened aureoles around granitic plutons emplaced along reactivated pre-existing faults. S_1, regional slaty-cleavage. Cf, Cleavage front. 1: Proterozoic basement. 2: Cambrian–Ordovician. 3: Silurian–Devonian. 4: Carboniferous. 5: Late Carboniferous granitic plutons (J, Jebilet, Ou, Oulmes, Z, Zaer).

Distribution of plutons

Many workers have observed that syntectonic plutons tend to be aligned along structural lineaments (Vigneresse & Brun 1983, Burg *et al.* 1984, Bussel & Pitcher 1985, Hutton 1988). At map-scale Moroccan plutons are aligned NE–SW parallel to the general trend of the belt. Autocorrelation analysis (Leymarie 1968, Fry 1979) also shows a good clustering along the NE–SW direction. Within clusters, however, plutons are distributed along ridges striking ENE–WSW and spaced 40–50 km apart (Fig. 3). The comparison of pluton distribution with map-scale lineaments shows that pluton alignments are parallel to NE–SW and ENE–WSW Proterozoic faults in the basement (Fig. 1), consistent with magma ascent along pre-existing deep faults. These faults were reacti-

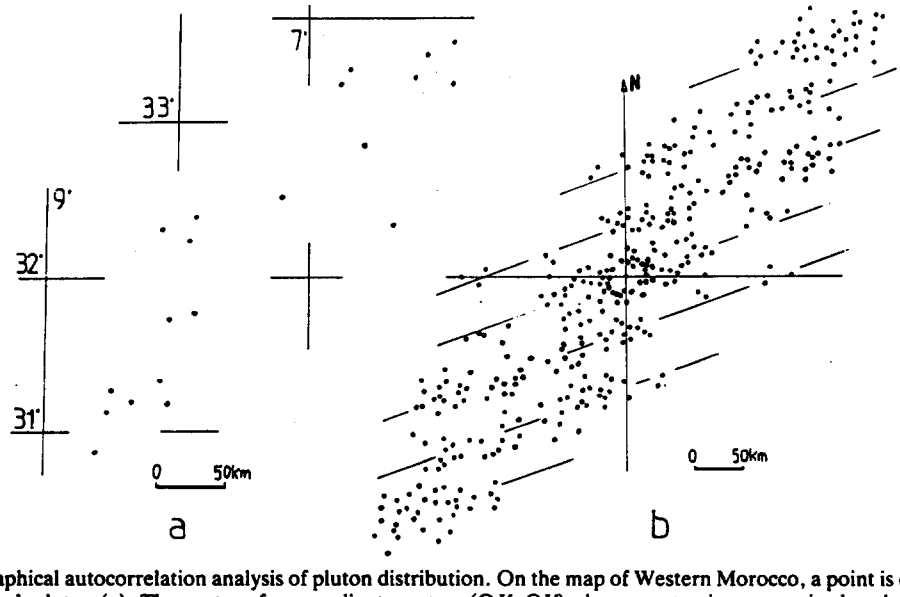

Fig. 3. Graphical autocorrelation analysis of pluton distribution. On the map of Western Morocco, a point is drawn at the center of each pluton (a). The center of a co-ordinate system (O*X*, O*Y*), drawn on tracing paper, is placed at one of the points on the map and the position of every other point (pluton center) is marked. The procedure is repeated for all points on the original map. The pattern which results (b) shows the frequency with which points on the map have neighbouring points at different distances in different directions (Leymarie 1968). Autocorrelation analysis confirms the clustering of Moroccan plutons along the NW–SE trend of the belt and shows that plutons are distributed along discrete ENE–WSW ridges spaced 40–50 km apart. Ridges are parallel to deep Proterozoic faults within basement.

vated in Hercynian time and formed the locus of both granite intrusions and shear displacements (Lagarde 1985) (Fig. 2).

Rows of plutons regularly spaced along ridges parallel to crustal faults are consistent with experiments which model the development of domes and plutons (Ramberg 1970, 1981). These experiments point out that the occurrence of discontinuities in source layers or overburden favours such localized magma ascent. Discontinuities control the formation of elongated domes which then give rise to spaced smaller-scale intrusions.

Shape of the plutons

The shape of the plutons is characteristic of the regional tectonic environment at the time of intrusion (Hutton 1988). Circular shapes are usual in post-tectonic or anorogenic intrusions (Bonin 1982). In contrast, the interference between pluton ballooning and regional simple shear can result in predominantly elliptical shapes (Brun & Pons 1981). Shape depends also on the ductility contrast between pluton and country rock (Ramberg 1970, Woidt 1978, Soula 1982).

In the Moroccan Hercynian belt, most pluton shapes can be approximated by NE–SW ellipses, whose principal axes (A) range from 9 to 40 km (Fig. 4). Local asymmetrical tear-drop shapes, indicating the sense of shear (Berthé *et al.* 1979), are observed in plutons directly bounded by ductile wrench faults (pluton 4, Figs. 1 and 4). Gravity data (Van den Bosch 1974, Bernadin 1988) indicate a 3–6.5 km vertical thickness for most of the plutons with a minimum value of 2 km for the deeply eroded Zaer granodiorite (Fig. 5). Pluton ellipticity (A/B) decreases as a function of emplacement timing (Fig. 6a) and axial ratios of pluton cross-sections are independent of the size of plutons (Fig. 6b).

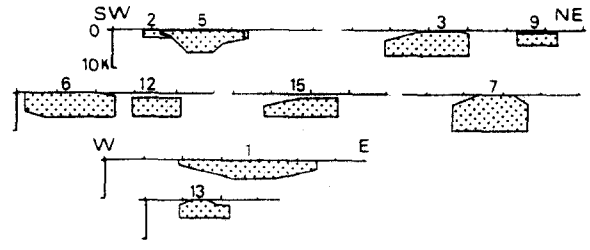

Fig. 5. Vertical shape and depth of pluton floors obtained from gravity data showing dominant tabular shapes (from Bernardin 1988) (pluton numbers as for Fig. 1).

Three basic pluton shapes can be distinguished from gravity and field data: flat plutons, tailed bubbles and discordant cauldrons (Fig. 7). These shapes are interpreted to be directly dependent on intrusion mechanism. Flat plutons are exemplified by the Eastern Jebilet granodiorite and the Zaer monzogranite (Chemsseddoha 1986, Diot 1989) (plutons 1 and 5, Fig. 1). They display gently outward-sloping contacts which are consistent with a high axial ratio in cross-section (Fig. 6b). Such relatively tabular shapes may be related either to vertical flattening of diapiric tailed globules when pluton

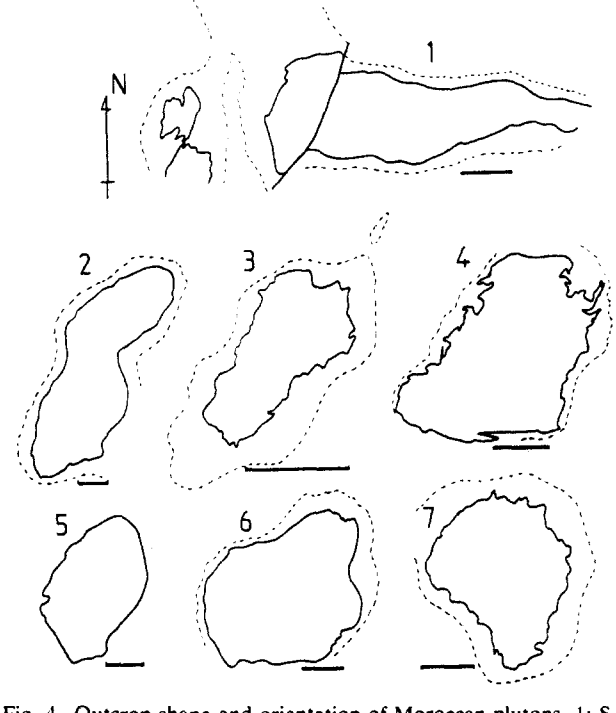

Fig. 4. Outcrop shape and orientation of Moroccan plutons. 1: S–I-type Jebilet granodiorite. 2: I–S-type Zaer granodiorite. 3: S-type Oulmes monzogranite. 4: I-type Tichka granitoid. 5: S-type Zaer monzogranite. 6: Rehamna alkaline monzogranite. 7: Ment granodiorite. Dotted lines: inner thermal aureole. Scale bar 5 km.

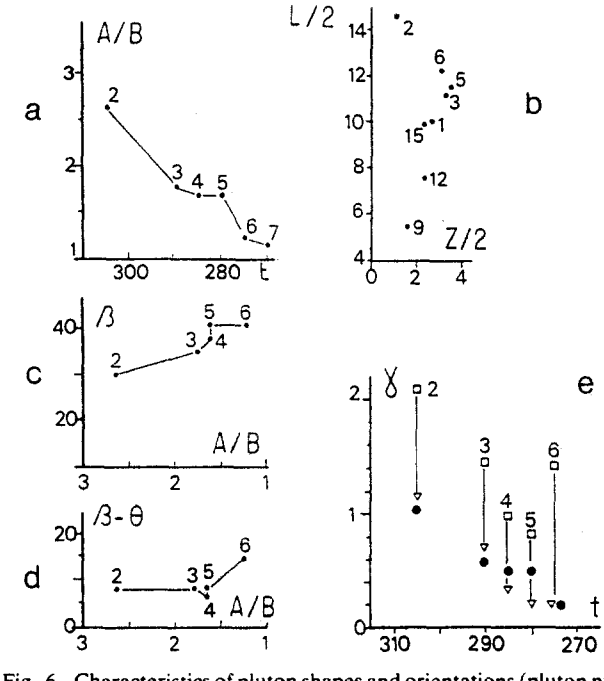

Fig. 6. Characteristics of pluton shapes and orientations (pluton numbers as for Fig. 1). (a) progressive decrease of pluton ellipticity (A/B) as a function of emplacement timing (t) in Ma. (b) diagram of computed long axis ($L/2$) (gravity data) vs depth ($Z/2$). (c) & (d) Pluton long axis obliquity to the regional ENE shear plane (β) and to the regional schistosity (β–θ), as a function of pluton ellipticity (A/B). Smaller obliquities correspond to high axial ratio of older plutons. (e) progressive decrease of the shear strain γ as a function of time (t) in Ma. Shear strain γ is registered by pluton shape (black circles) and by pluton obliquity (β) (triangles). Regional shear strain (squares) is registered by schistosity obliquity to the regional shear plane (θ). The difference between strain registered by plutons and the bulk strain is related to the delay of pluton emplacement with respect to the beginning of regional deformation.

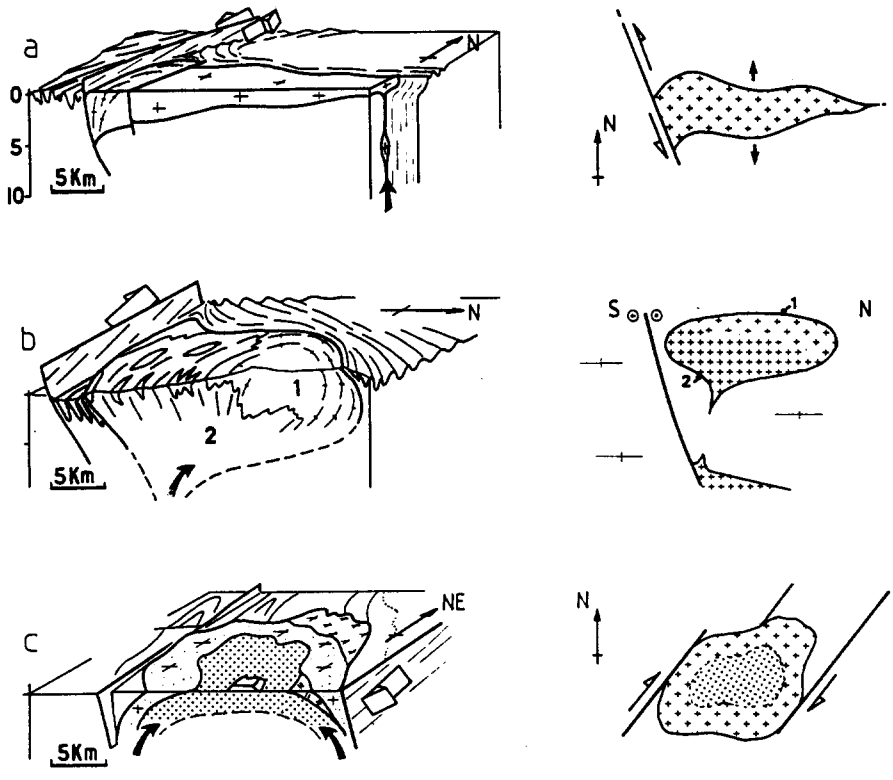

Fig. 7. Three-dimensional shapes of Moroccan plutons and related emplacement mechanisms. (a) Tabular shape (eastern Jebilet pluton) compatible with pluton emplacement along an extensional E–W fault in a shear zone termination. (b) Tailed globule shape (Tichka pluton) consistent with a diapiric ascent inducing a strong deformation of adjacent country rocks (1, granitoids; 2, diorites and gabbros). Asymmetric pluton shape (northwards offcentred acidic roof) suggests that pluton did not rise vertically. (c) Concentric flat-lying sheets of alkaline granites (Rehamna) indicating local cauldron subsidence and pull apart along a major crustal wrench fault (Western Meseta shear zone).

ascent is stopped, or to emplacement by multiple pulses of magma along crustal fractures leading to *in situ* assembled plutons. The long and narrow Jebilet granodiorite is thought to be emplaced along a pre-existing E–W crustal discontinuity by wedging into weakly deformed country rocks, giving rise to a tongue-shaped flat pluton (Fig. 7a).

Tailed bubble shapes are exemplified by the Tichka pluton (pluton 4, Fig. 1) which shows an inward-dipping floor and an outward-sloping roof (Termier & Termier 1971) (Fig. 7b). The diapiric emplacement of this pluton is supported by (i) the large deformed aureole with numerous peripheral buckle folds, (ii) strain patterns (foliation trends, down-dip stretching lineation, decrease of strain outside the aureole) and (iii) strain kinematics indicating the rise of the magma relative to its outer margins (Lagarde & Roddaz 1983). The three-dimensional asymmetric shape of the Tichka intrusion (eccentric foliation trends, northward offcentered acidic roof), suggests that the pluton did not rise vertically (Talbot 1977) and may further indicate a northward inclined melting source interface (Talbot 1974) (Fig. 7b). Such inclination is consistent with the southward thrusting combined with dextral wrench faulting along the Tizi n'Test Fault (Mattauer *et al.* 1972, Petit 1976).

Discordant cauldrons are exemplified by the flat-lying sheets of alkaline granite (Azegour and Rehamna intrusions, 6 and 8 on Fig. 1). They display flat roofs, steep sides, concentric patterns, fracturing of the roof and block subsidence (Lagarde 1987) and are compatible with pull-apart and local subsidence along large-scale fractures (Fig. 7c).

Pluton orientations

Many syntectonic plutons are oriented with respect to the regional strain field (Brun & Pons 1981, Hutton 1982, 1988). Pluton orientations are usually described by the obliquity of pluton long axis with respect to the regional shear plane (β) and to the regional schistosity (β–θ) (Vigneresse & Brun 1983).

In Western Morocco, pluton long axes are oriented in a NE–SW direction, subparallel to the regional trend of the belt. This orientation is consistent with a regional NW–SE shortening during pluton emplacement. The transverse orientation of the E–W Jebilet granodiorite is an exception compatible with pluton emplacement along an extensional E–W fault in a shear zone termination (Fig. 7a). Pluton long axes are clearly oblique to the regional ENE shear plane (β values) and slightly oblique to the regional NE–SW schistosity (β–θ) (Figs. 6 b & c). This obliquity suggests that plutons are less reoriented towards the regional shear plane than is the schistosity. In terms of regional shear strain, γ, this angular obliquity corresponds to a difference of about 0.5–1 γ between the regional strain and the local strain recorded by plutons (Fig. 6e). Lower obliquities (β) are observed for higher axial ratio of older plutons, i.e. older plutons are less oblique to the regional shear plane than are younger ones.

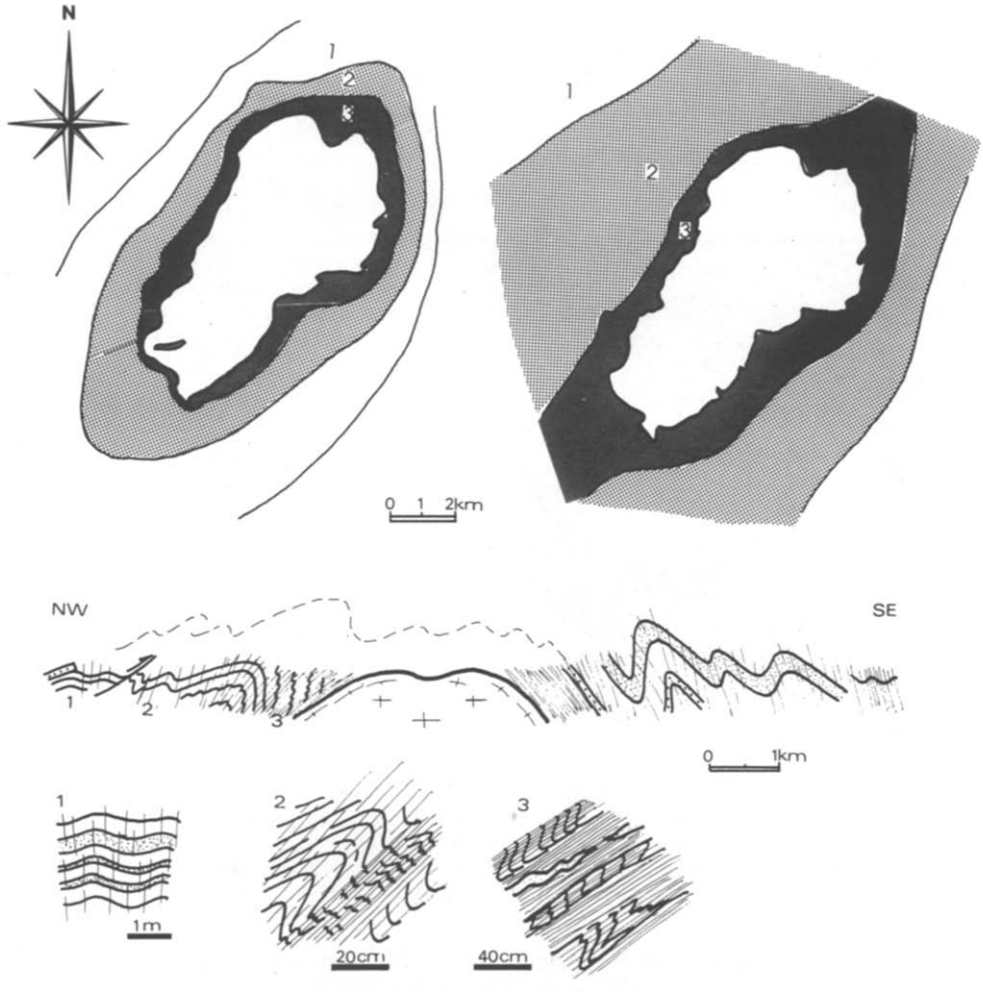

Fig. 8. Deformation patterns and microstructural evolution around the Oulmes monzogranite. (a) Thermal aureole centered on the pluton. 1: muscovite–chlorite zone. 2: Biotite zone. 3: Biotite–andalusite ± cordierite, garnet, sillimanite zone. (b) Typologic evolution of schistosity. 1: Discrete cleavage S_1. 2: Slaty cleavage S_1. 3: Composite foliation S_{1-2}. (c) Cross-section showing progressive strain increase towards pluton and evolution from weakly developed cleavage (S_1), axial planar to upright open F_1 folds (1), to composite S_{1-2} foliation axial planar to asymmetric folds verging towards pluton (2) and (3).

Distribution and microstructural evolution of the deformation in country rock

The Western Moroccan Hercynian belt is weakly deformed. Deformation consists of a faintly developed schistosity (S_1), axial planar to NE–SW gently-plunging folds. This main regional deformation increases near plutons as a result of heating and hydrolitic weakening of country rock and there is a close correspondence between areas of pluton emplacement and deformed zones (Fig. 2).

Plutons control the microstructural evolution in the surrounding rocks. This evolution is characterized by the progressive development of superimposed small-scale structures and can be observed around most of the plutons studied (Zaer and Oulmes monzogranites, and Zaer, Tichka and Jebilet granodiorites). In the outermost zones of the aureoles ductile deformation initiated by the development of a weak steeply-dipping cleavage (S_1) that is axial planar to upright, open and gently-plunging F_1 folds (Figs. 8c and 9a). Closer to the contact, the bedding S_0 is progressively transposed into the S_1 cleavage. Asymmetric F_1 folds verge towards the plutons (Fig. 8c). In the innermost zones of the aureoles (0.5–1 km) deformation increases strongly. S_1 cleavage and bedding are deformed by F_2 folds with S_2 axial plane foliation. Away from F_2 fold hinges, S_1 and S_2 are parallel and form a composite S_{1-2} foliation accompanied by the growth of contact metamorphic porphyroblasts.

Where plutons are directly bounded by a regional shear zone, as in the Jebilet massif, the strain intensity is still higher. F_2 folds are strongly sheared in the S_{1-2} composite foliation. F_2 fold axes curve in the shearing plane and rotate towards the stretching direction giving rise to a great variation in plunge (Fig. 11b). In the most highly sheared zone, only F_2 fold hinges are preserved (Fig. 9b). The S_{1-2} foliation is deformed by F_3 conjugate kink folds (Berthé & Brun 1980), symmetrically disposed about the stretching direction and consistent with a sinistral sense of shear (Fig. 11). A third cleavage develops locally. It consists of S_3 shear bands indicating extension parallel to S_{1-2} in a non-coaxial regime (Platt & Vissers 1980). This microstructural evolution leading

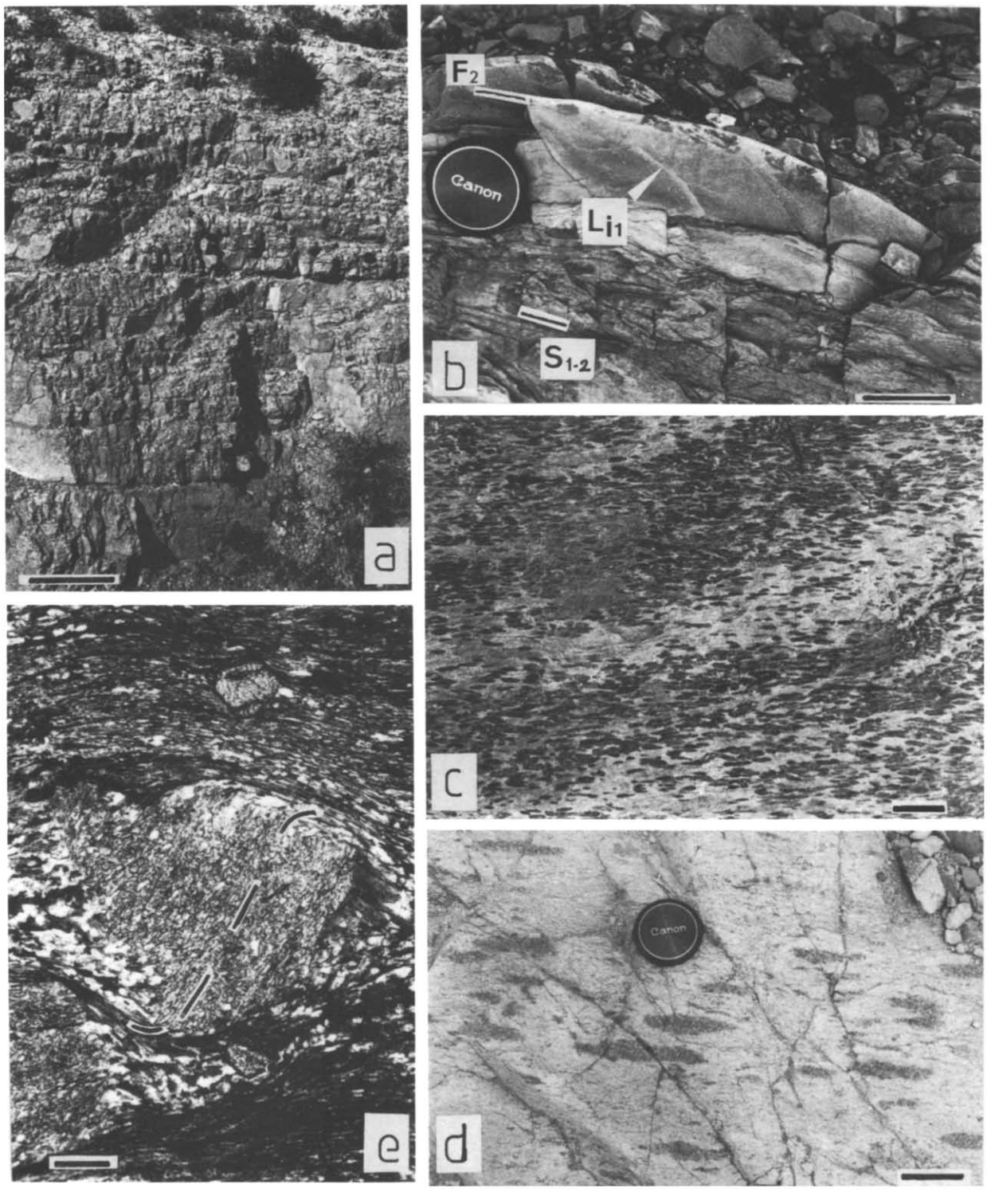

Fig. 9 Microstructural evolution of the deformation. (a) Axial planar discrete cleavage (S_1) (outer aureole of the Oulmes pluton). (b) L_{i1} intersection lineation deformed by a fold (F_2) strongly sheared in the S_{1-2} composite foliation (inner aureole of the Jebilet pluton deformed along the Marrakech shear zone). (c) Elliptical strain markers (elongated contact metamorphic spots of cordierite, $\lambda_1\lambda_2$ section) within thermal aureoles. (d) Strain markers in granites (dark aggregates of quartz–tourmaline, monzogranite dykes, Jebilet pluton). (e) Photomicrograph in crossed nicols of syntectonic andalusite porphyroblasts with rotated inclusion trails (Jebilet pluton aureole). Scale bars for (a) 50 cm, (b) & (d) 5 cm, (c) 2 cm, (e) 500 μm.

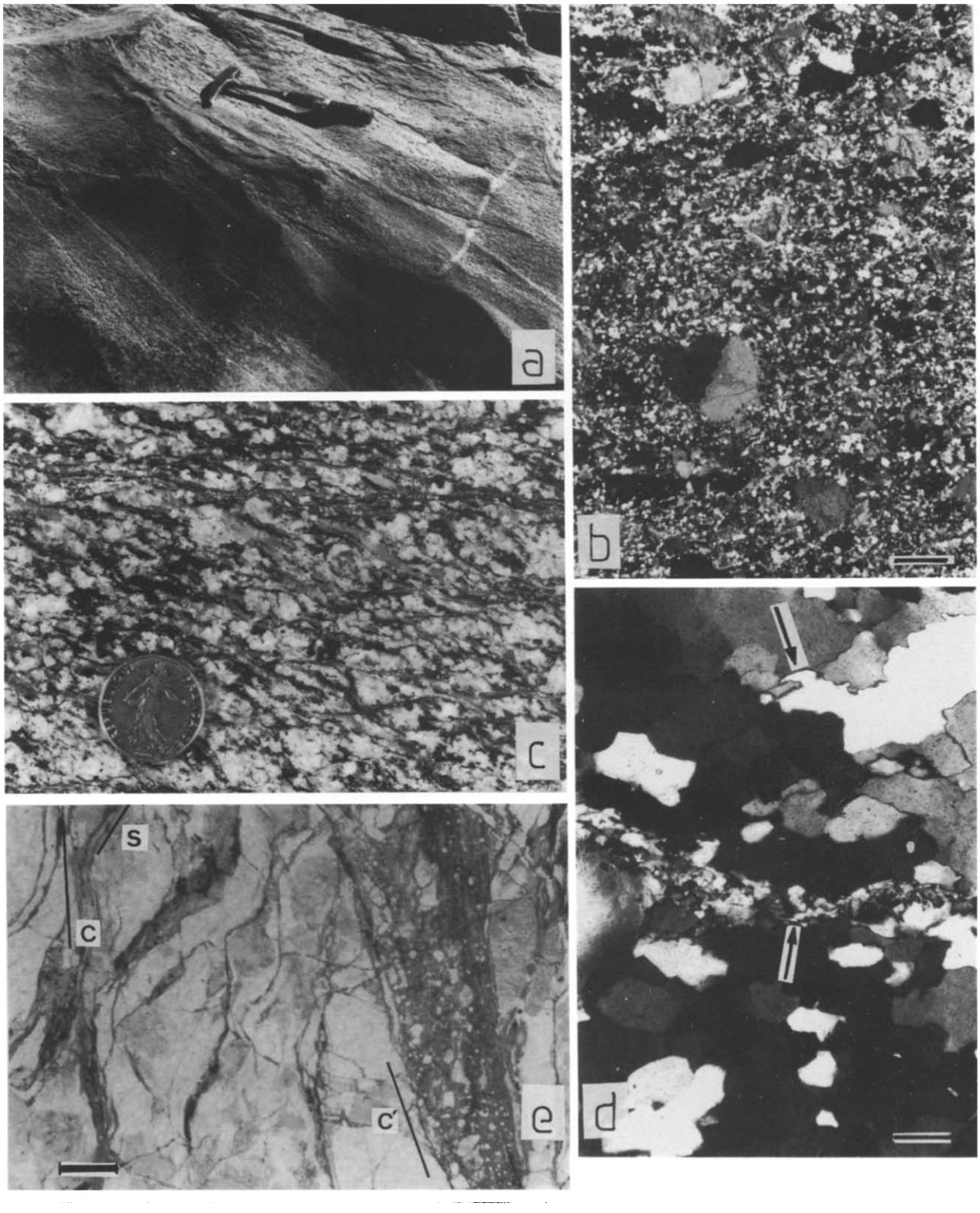

Fig. 10. Foliation development in granitoids. (a) High-temperature orthogneisses with homogeneous penetrative foliation (Oulmes monzogranite). (b) Photomicrograph with nicols crossed of high-temperature solid-state foliation in Oulmes monzogranite showing typical fine-grained quartz–feldspar matrix, with no clear shape or crystallographic fabrics. (c) *C–S* orthogneisses characterizing a heterogeneous, medium-temperature solid-state deformation (Jebilet granodiorite). (d) Photomicrograph with nicols crossed of initiation of *C*-surfaces within a *C–S* orthogneiss (Jebilet granodiorite). *C*-surface is composed of fine-grained quartz–feldspar ± mica aggregates concentrated along an imperfectly defined plane (lower arrow). Note that adjacent quartz grains display characteristic lobate shapes (upper arrow) which reveal extensive grain boundary migration. (e) Photomicrograph in plane light of cataclasites developed along discrete synthetic shear planes, *C'*, characterizing brittle shallow crustal conditions (*C–S* orthogneiss, Jebilet). Scale bars for (b) & (d) 300 μm and (e) 2 mm.

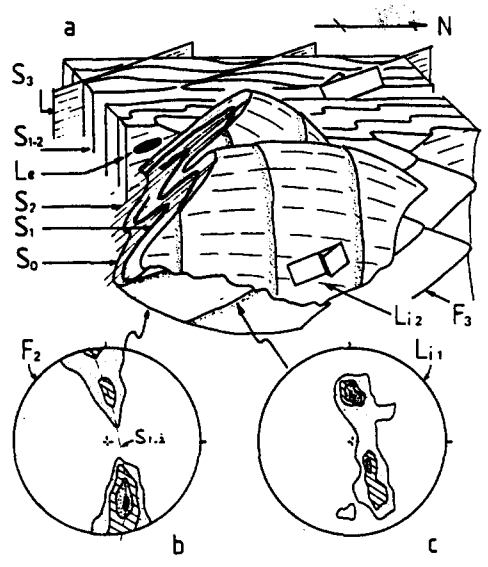

Fig. 11 Superimposed microstructures across a strongly sheared pluton aureole (Marrakech shear zone). (a) Sketch depicting bedding (S_0), superimposed cleavages (S_1, S_2, S_{1-2}, S_3), folds (F_2, F_3), intersection lineations (L_{i1}, L_{i2}), stretching lineation L_e). (b) F_2 fold axis dispersion resulting from shearing along the S_{1-2} foliation (shear direction plunges slightly to the south) (n = 110, contour intervals at 1, 5, 10 and 24%). (c) Dispersion of the L_{i1} intersection lineation on the F_2 folds (n = 55, contour intervals at 2, 10, 12 and 20%).

to local refolding and complex lineation patterns is related to a progressive deformation (Lagarde & Choukroune 1982).

Strain intensity patterns

The influence of pluton emplacement on strain intensity patterns may be estimated by finite strain measurements made on elliptical deformed objects (Fig. 12). Most of these deformed objects initially had a subspherical form (metamorphic spots of cordierite and reduction spots within country rock; aggregates of quartz-tourmaline within granitic rocks) (Figs. 9c & d). Determinations of the ellipses were made by direct measurement and data are represented on a graph of long vs short axes (Ramsay 1967). Where fluctuations in orientation of the long axes are detected, indicating an initial ellipticity, computations followed the R_f/ϕ method (Dunnet 1969). Estimation of strain intensity is obtained from r parameter computation (Watterson 1968). The preferred orientation of micas, measured by X-ray texture goniometry, is quantified by a fabric intensity index R_f (Le Corre 1978) which shows the same variations as the r parameter.

Strain intensity patterns show the following characteristics.

(1) Within country rocks, strain intensity profiles show a progressive increase towards pluton boundaries (Fig. 13a). This strain increase is consistent with the observed microstructural evolution and the tightening of folds in the aureole. Highest strain intensities occur near pluton margins that are strongly sheared along regional transcurrent shear zones (Fig. 13b). Lower strain intensities occur in well developed hornfels and in the envelopes of the discordant intrusions (Fig. 13c).

(2) Within plutons, strain is generally low but increases towards pluton margins (Fig. 13a). A good assessment of this strain increase is also given by the microtextural evolution from non-foliated granites to protomylonites and *C–S* mylonites (Fig. 14). This evolution emphasizes that strains concentrate in the outer parts of plutons, but the lack of peripheral ultramylonites and the rather low values of strain measured in these zones (Fig. 13a) are not compatible with a strong lateral expansion of plutons. Ultramylonites are well developed in plutons emplaced in zones with high regional shear strain (central and eastern Jebilet plutons) (Fig. 14a). They cut across peripheral *C–S* mylonites and display an asymmetrical pattern, discussed below.

Strain intensity patterns have been successfully used to estimate the relative timing of intrusion and deformation (Brun & Pons 1981, Hutton 1982). Where pluton emplacement occurs after the beginning of the regional deformation, pre-tectonic markers such as reduction spots record the bulk strain of country rocks, whereas pluton related markers such as metamorphic spots only record strain increments since pluton emplacement. Strain profiles using strain markers introduced during pluton emplacement (contact metamorphic spots) will therefore indicate lower intensities than strain profiles using pre-tectonic markers. Comparison of strain profiles around the Azegour alkaline intrusion exemplify this delay of pluton emplacement in comparison with the beginning of the regional deformation (Fig. 13c), emphasizing the late tectonic emplacement of the discordant alkaline intrusions of Morocco.

Variations of strain ellipsoid shapes

Strain ellipsoid shapes are described by the k parameter (Flinn 1962). Around Moroccan plutons, k values range from 0.1 to 8.7 suggesting significant changes in strain ellipsoid shapes (Fig. 12d).

In country rocks, the k value progressively decreases towards plutons indicating a progressive increase of flattening ($0.1 \leq k < 1$). Deformed pluton margins also display oblate strain ellipsoids (field circled a on Figs. 12d and 13a). This progressive flattening is consistent with microtectonic observations such as chocolate-tablet boudinage of competent layers and with the strong planar fabrics of micas measured by X-ray texture goniometry (Chemsseddoha 1986). A strong flattening strain around plutons is predicted both by mathematical models of interference between regional simple shear and pluton ballooning (Brun & Pons 1981) and by the analysis of deformation around a rising diapir modeled by creeping flow past a rigid sphere (Cruden 1988).

At the extremities of plutons, the k value increases. A constriction type strain ($1 < k < 5$) develops in these zones (field circled c on Figs. 12d and 13a). The change in strain ellipsoid shape is accompanied by a change of fabric from $L < S$ tectonites to $S < L$ tectonites.

Plane strain ellipsoids are measured within shear zones. Where shear strain increases, finite strain measurements indicate an evolution from plane to pro-

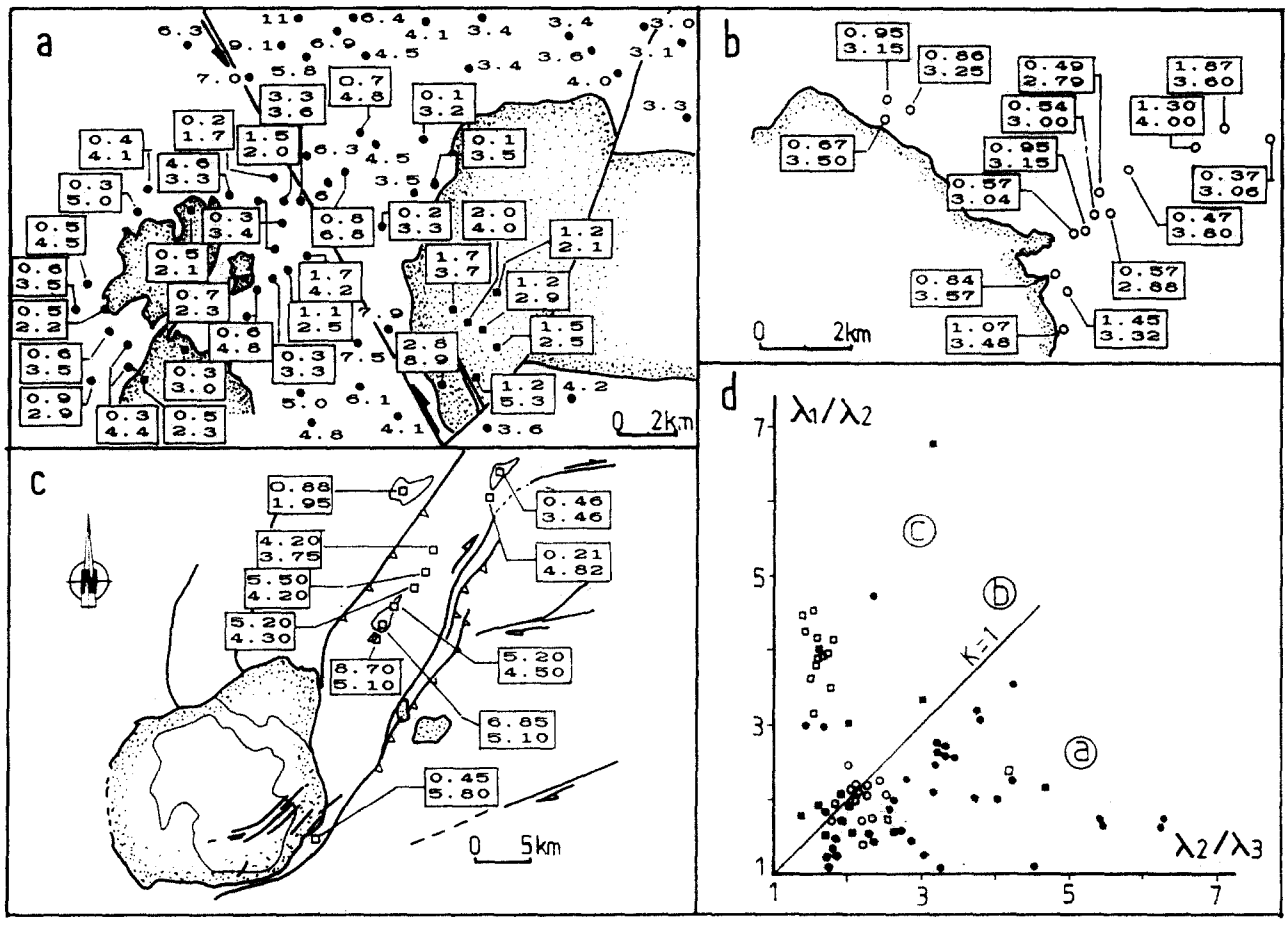

Fig. 12. Finite strain measurements. In (a), (b) & (c) boxes contain k (upper) and r (lower) values, where $r = \lambda_1/\lambda_2 + \lambda_2/\lambda_3 - 1$. (a) Data from syntectonic Jebilet pluton (squares) and its aureole (filled circles). Unboxed data are R_f (fabric intensity index) values. (b) Data from aureole of late tectonic Azegour intrusion. (c) Data from high strain rocks of Rehamna thrust-wrench shear zone. (d) Flinn plot of data from (a) (b) and (c) showing dominantly flattening-type strain ($0 \leq k < 1$) in aureoles and plutonic rocks (circled a), a slight trend towards plane strain ($k \simeq 1$) related to measurements along shear zones (circled b), and an evolution to constriction type strain ($k > 1$) in schistosity triple points (Jebilet) and zones of high shear strain (Rehamna). 25–150 strain measurements per symbol.

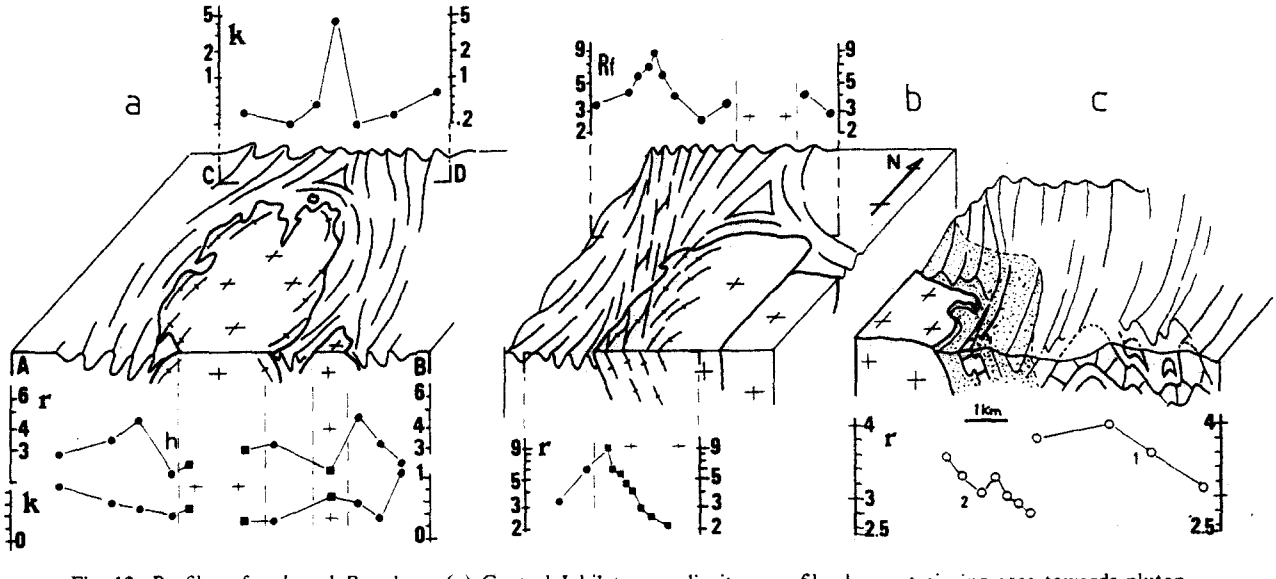

Fig. 13. Profiles of r, k and R_f values. (a) Central Jebilet granodiorite r profile shows strain increase towards pluton boundaries and low strain in pluton core and peripheral hornfels (h). k profiles show dominantly oblate strain (AB section) evolving to prolate strain in schistosity triple point (CD section). (b) Eastern Jebilet granodiorite. Highest strain intensities on r and R_f profiles occur across pluton margins deformed along regional shear zones. (c) Late tectonic Azegour monzogranite. Right-hand r profile from pretectonic strain markers (reduction spots) records bulk regional strain. Left-hand r profile from contact metamorphism spots records strain accumulated since pluton emplacement.

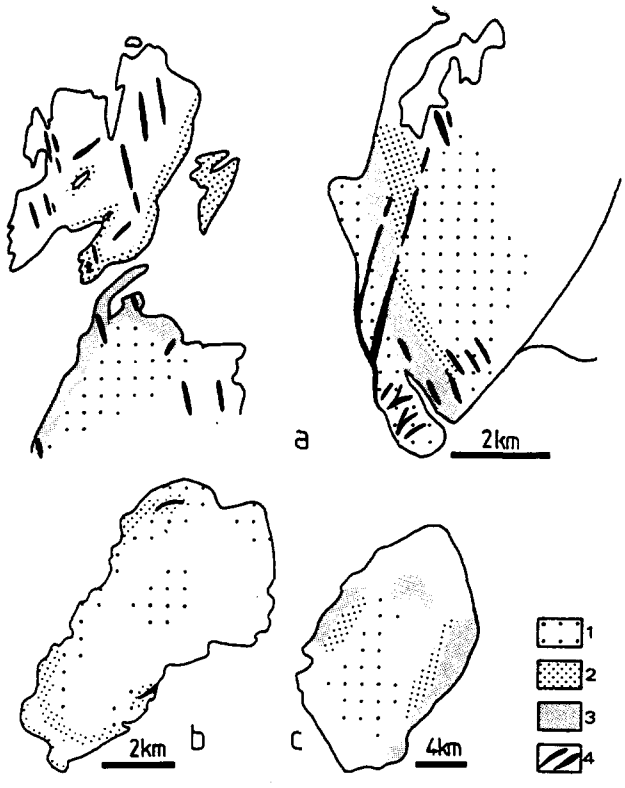

Fig. 14. Patterns of internal microstructures. (a) Central and eastern Jebilet granodiorites. (b) Oulmes monzogranite. (c) Zaer monzogranite. 1, Weakly deformed zones with discrete *S*-surfaces; 2, *C–S* protomylonites with dominant *S*-surfaces; 3, *C–S* mylonites with dominant *C*-surfaces; 4, ultramylonites.

late finite strain (Lagarde & Michard 1986) (fields circled b and c on Fig. 12d).

Finite strain trajectories

Finite strain trajectories (flattening plane and λ_1 orientations) reflect the orientation of the strain ellipsoid axis. In Western Morocco patterns of finite strain trajectories emphasize the synchronism between aureole structures, internal structures of plutons and regional structures. The aureole foliation shows a geometrical continuity with the regional schistosity (Figs. 15c and 16a) and structures of the aureole are not overprinted on regional structures. Trends of pluton foliations are generally continuous with those of the aureole suggesting a rather low ductility contrast between the pluton and the inner aureole. Where schistosity is lacking outside the thermally softened areas, the boundaries of the aureoles show a foliation oriented NE–SW, conformable to the regional strain field (Figs. 15a & b). Most stretching lineations of the aureoles present rectilinear patterns oriented in the direction of regional stretching. The only observed curvatures of the lineation trends are related to transcurrent shear zones (Fig. 16a).

Perturbations of the strain field, related to pluton emplacement, can be detected on the maps of finite strain trajectories. In the innermost parts of the aureoles, fold axes and foliations tend to become parallel or slightly oblique to the contact of the pluton. They form curved or elliptical trend lines contrasting with the rectilinear trends observed farther out. Internal helicoidal foliations show a regular sense of obliquity with respect to pluton boundaries (Fig. 15b). Foliation triple points develop at the extremities of plutons. They correspond to weakly deformed triangular zones where a foliation parallel to pluton interface initiates at a high angle to the NE–SW foliation. In these zones both foliations are, in turn, locally shortened and crenulated, consistent with their synchronous development. Foliation triple points have been explained in terms of interference between pluton ballooning and simple shear (Brun & Pons 1981).

At the top of plutons, internal stretching lineations do not follow the foliation curvature but are slightly plunging and strike NE–SW parallel to pluton long axes (Figs. 15a & b). Near the inward-dipping floor of tailed plutons stretching lineations become down-dip and display radial patterns (Fig. 15c).

Syn-tectonic contact metamorphism

The heating of the aureoles by heat loss from the magma, gave rise to a contact metamorphism showing the following characteristics.

(1) Thermally softened aureoles around plutons are usually 1–2 km wide. They are characterized by low-pressure andalusite–sillimanite metamorphism indicating high geothermal gradients. Aureoles are centered on granitoids and metamorphic zonations consist of three main zones: muscovite–chlorite zone, biotite zone and andalusite–cordierite zone (±sillimanite, garnet) (Fig. 8a)

(2) Contact metamorphism porphyroblasts show a syntectonic growth with respect to the foliation. Andalusite exhibits sigmoidal inclusion trails (Fig. 9e). A post-tectonic growth of contact porphyroblasts as biotite and andalusite is locally observed, which indicates that thermal relaxation outlasted deformation of the country rocks.

(3) Where plutons were emplaced along a regional shear zone, the rotation of contact porphyroblasts is consistent with the regional sense of shear (Chemsseddoha 1986).

The metamorphism in the aureoles contrasts strongly with the upper epizonal metamorphism associated with the regional deformation (Piqué 1982). K–Ar dating (Huon 1985) shows that regional metamorphism minerals in slates and igneous minerals in granitoids (Mrini 1985) are comparable in age. This emphasizes that regional schistosity and pluton foliation are synchronous and developed during pluton emplacement.

Foliation development in granitoids

Data presented above provide evidence for pluton emplacement during regional deformation: internal foliations are continuous with regionally developed cleavages; porphyroblasts in the contact aureoles are syntectonic with respect to the foliation; magmatic and

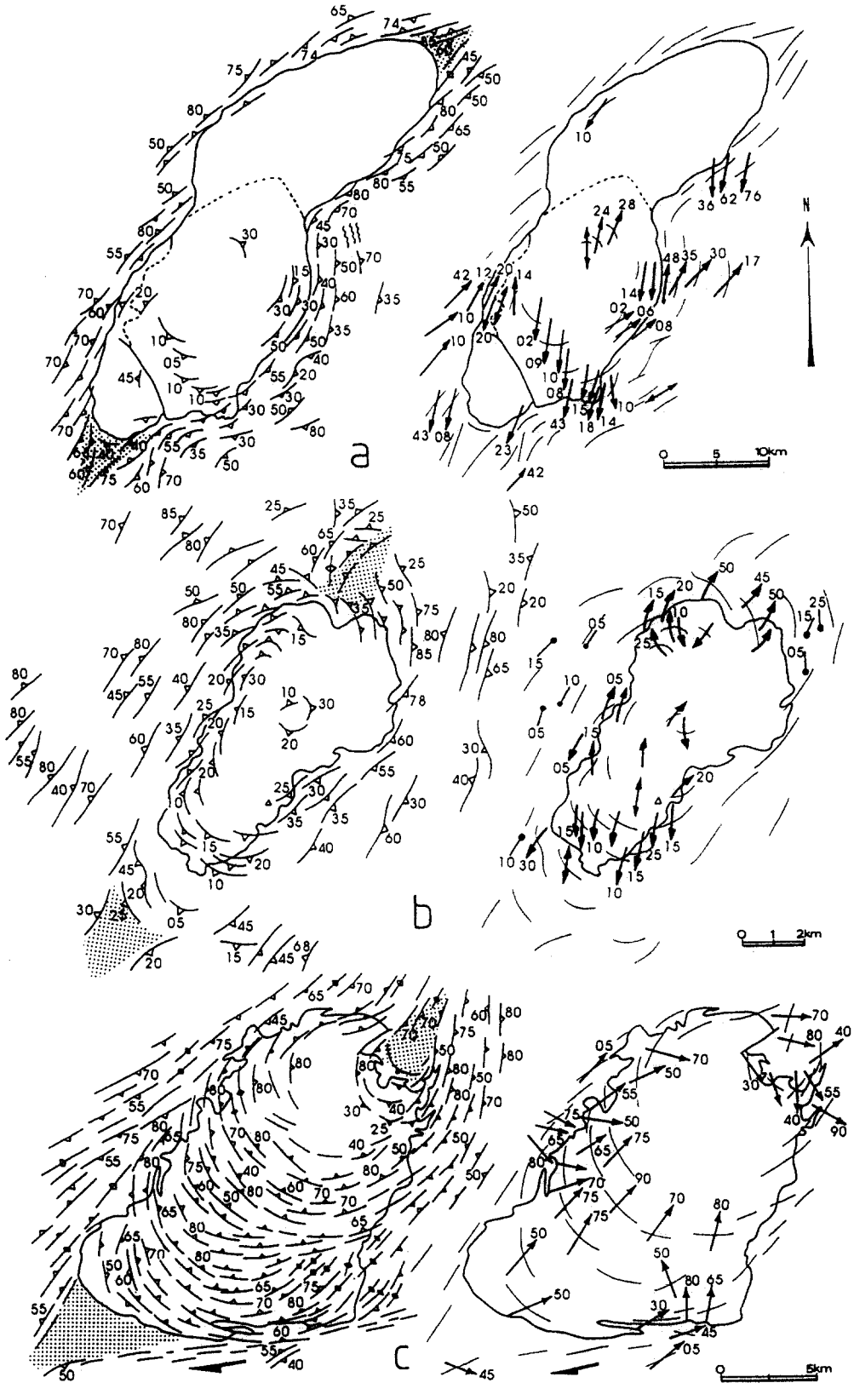

Fig. 15. Foliation (left) and stretching lineation (right) maps. (a) Zaer. (b) Oulmes. (c) Tichka. Foliations are characterized by (i) a dominant NE–SW orientation, (ii) a geometrical continuity between aureole and pluton foliations leading to elliptical trend lines, (iii) foliation triple points (dots) at the extremities of pluton ellipses and (iv) helicoidal pattern in (b) compatible with transcurrent motion. Stretching lineations display (i) rectilinear trends parallel to the regional stretching (a & b) and (ii) radial patterns near the inward-dipping floor of the Tichka granitoids (c).

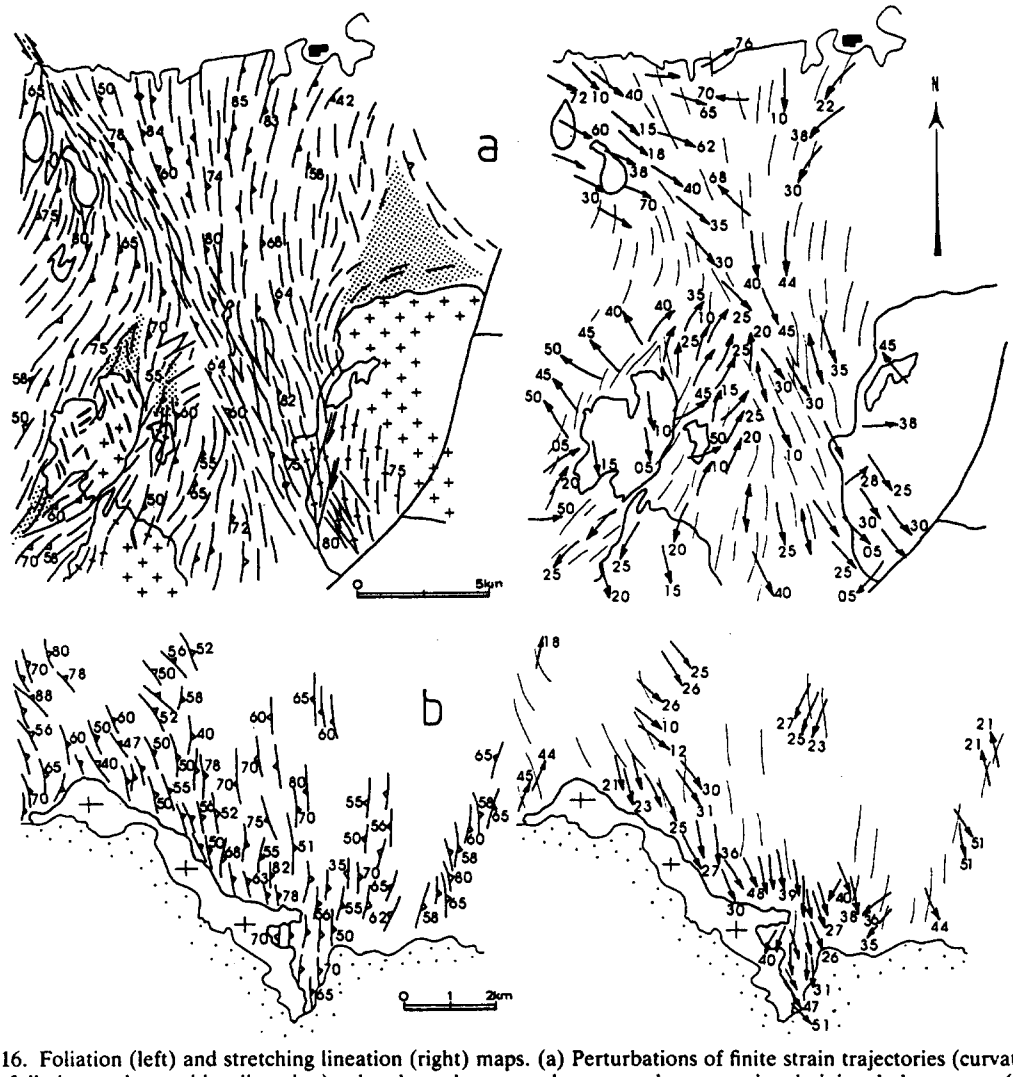

Fig. 16. Foliation (left) and stretching lineation (right) maps. (a) Perturbations of finite strain trajectories (curvature of both foliation and stretching lineation) related to pluton emplacement along a regional sinistral shear zone (Jebilet granodiorites). (b) Finite strain trajectories around a late tectonic intrusion (Azegour monzogranite). Granitic intrusion cuts across regional foliation but stretching direction near granite, indicated by elongated contact metamorphism spots, is conformable to the regional stretching direction.

metamorphic minerals have similar age. Another strong piece of evidence is the development of internal foliation during pluton emplacement (Gapais 1987, Blumenfeld & Bouchez 1988, Paterson *et al.* 1989). This latter point is supported by two basic features, each being diagnostic of syntectonic emplacement. The first feature is the occurrence of microstructures developed during the high-temperature stage of pluton emplacement. The second feature is the occurrence of microstructural variations recording the decrease in temperature accompanying pluton cooling.

High-temperature microstructures are preserved where intrusive effects predominate and are not overprinted by lower temperature regional effects (Oulmes and Zaer monzogranites). High-temperature orthogneisses are located near pluton–country rock interfaces. They display homogeneous penetrative foliations (Fig. 10a) and shear bands are unusual (Ait Omar 1986). At the microscale, orthogneisses consist of a homogeneous matrix including small quartz and feldspar grains with no clear shape fabric (Fig. 10b). The crystallographic orientation of quartz grains is very slight suggesting a progressive reorientation and misorientation of subgrains (Poirier & Nicolas 1975, Simpson 1983). Such a fabric is consistent with high crystallization rate during the high-temperature history of syntectonic pluton emplacement (Gapais 1987). No clear microstructural evidence of magmatic flow (suspension-like behaviour) (Paterson *et al.* 1989) can be found in these zones and the observed foliations reflect only high-temperature solid-state flow (subsolidus plastic deformation) (Gapais 1987, Paterson *et al.* 1989).

Microstructural variations recording the progressive decrease in temperature associated with pluton cooling are observed where regional deformation effects are well developed and outlast the high-temperature history of pluton crystallization. In the eastern Jebilet granodiorite, which is strongly sheared along a regional transcurrent SSE shear zone, increasing strain is marked by the transition from an originally non-foliated granite to typical *C–S* mylonites and ultramylonites (Lagarde & Choukroune 1982). Microstructural changes that occur during this progressive foliation development may be summarized as follows.

(1) *C–S* structures initiate by the association of a weak schistosity (*S*-surfaces) and of small ductile shear bands (*C*-surfaces). Shear bands consist of small aggregates of quartz, feldspars and biotites concentrated along imperfectly defined planes (Fig. 10d).

(2) Increasing strain, indicated by finite strain measurements (Fig. 13b), is marked by propagation and amplification of shear bands (Fig. 10c) during unstable solid-state flow. Quartz, feldspars and micas experience internal deformation, grain size reduction and recrystallization within shear bands. Quart grains exhibit some lobate shapes indicating that grain boundary migration processes are still active (Gapais & Barbarin 1986). Quartz fabrics are characterized by (i) the development of ⟨*a*⟩ axes concentrated close to λ_1, (ii) ⟨*c*⟩ axes distributed within asymmetric crossed-girdles with a maximum close to λ_2 (Fig. 17), (iii) an asymmetry (Lister & Williams 1979) consistent with the sense of shear indicated by shear bands. The fabrics developed at relatively low temperature by dominant ⟨*a*⟩ slip and rotation–recrystallization deformation mechanisms (Gapais & Barbarin 1986). The evidence of quartz grain boundary migration indicates, however, a temperature of deformation around the migration–rotation recrystallization transition (≈550°C) (Gapais 1987).

(3) A further decrease in pluton temperature is accompanied by the development of cataclasites concentrated along discrete synthetic shear planes (*C'*) (Berthé *et al.* 1979), consistently inclined at 20–30° from the *C*-planes (Fig. 10e). In these cataclasites clusters of feldspars, biotites and polycrystalline quartz grains experienced a strong grain size reduction concomitant with an alteration of feldspars and biotites. This cataclastic process characterizes brittle shallow crustal conditions (Sibson 1977). The observed microstructural evolution implies that quartz is stronger than weakened feldspars and would indicate low-temperature deformation (<350°C) (Evans 1988).

The above observations emphasize that the Jebilet granodiorites have been emplaced and cooled during regional shearing. Microstructures recording the syntectonic cooling range from intermediate-temperature shear bands (≈550–600°C) to low-temperature *C'* cataclastic shear planes (<350°C) formed at the end of the thermal re-equilibration of plutons.

RELATIVE EFFECTS OF INTRUSION AND REGIONAL DEFORMATION

The relative effects of intrusion and regional deformation control the geometry and the kinematics of deformation in zones of syntectonic pluton emplacement. Geometry and kinematics are deduced from analysis of strain patterns (Brun & Pons 1981, Hutton 1982, 1988, Courrioux 1987) and from shear criteria (Berthé *et al.* 1979, Simpson & Schmid 1983, Burg 1987, Blumenfeld & Bouchez 1988). They provide good indications of the tectonic environment during final emplacement of plutons (Fig. 18).

Where regional effects are prominent and outlast high-temperature deformation history of plutons, intrusive effects are not clearly registered and strain patterns are mainly controlled by the regional wrenching (eastern Jebilet granodiorite) (Fig. 18a).

Where weak intrusive effects interfere in the regional strain field, a peripheral fabric develops in granites, but without conspicuous registering of the upward motion of

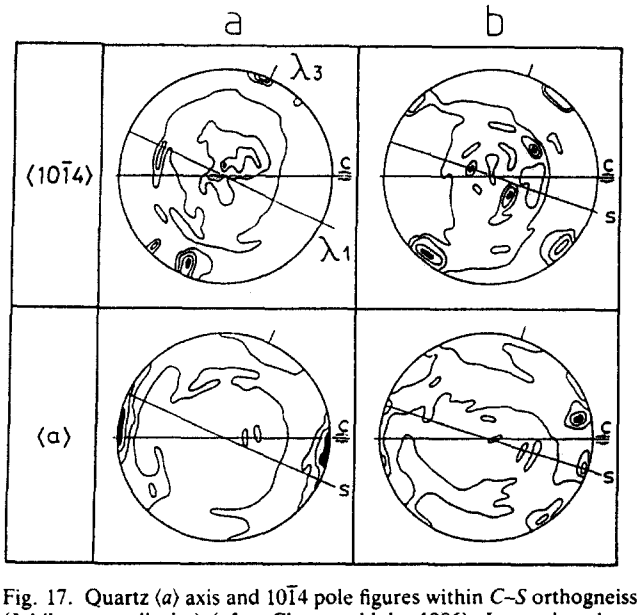

Fig. 17. Quartz ⟨*a*⟩ axis and 10$\bar{1}$4 pole figures within *C–S* orthogneiss (Jebilet granodiorite) (after Chemsseddoha 1986). Increasing shear strain from (a) to (b) is marked by the progressive concentration of ⟨*a*⟩ axes close to λ_1 and by the distribution of ⟨10$\bar{1}$4⟩ in asymmetric crossed-girdles. 10$\bar{1}$4 pole figures contoured at 1, 2, 3 and 4 times uniform distribution (u.d.). ⟨*a*⟩ axis figures contoured at 1, 2, 2.5 and 3 times u.d.

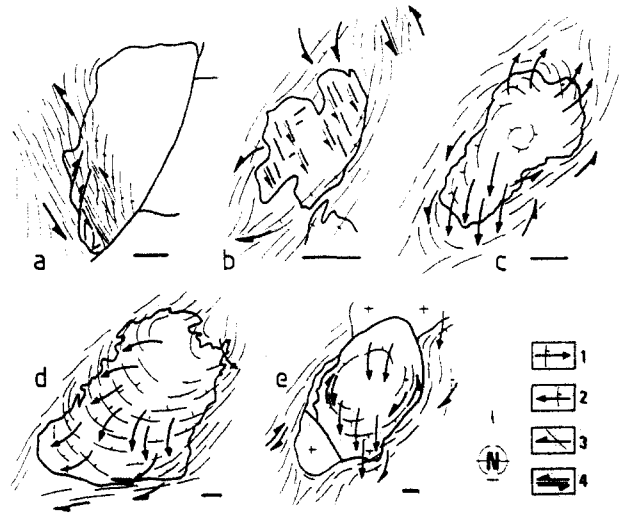

Fig. 18. Relative effects of intrusion and regional deformation deduced from strain patterns and shear criteria. (a) Eastern Jebilet granodiorite. (b) Central Jebilet granodiorite. (c) Oulmes pluton. (d) Tichka granitoids. (e) Zaer monzogranite. (a) & (b) Strain patterns controlled by a prominent regional wrenching. (c) & (d) show the combination of intrusive effects (peripheral orthogneisses, normal or reverse shears related to pluton ascent) and regional effects (NE–SW foliations with helicoidal or signoidal pattern, lateral wrenching). (e) shows predominantly intrusive effects (peripheral flat lying foliations with concentric patterns, southward sense of shear) consistent with southwards spreading of a flat pluton. 1: Normal shears. 2: Reverse shears. 3: Normal or thrust-wrench shears. 4: Wrench shears.

the magma (central Jebilet granodiorite) (Fig. 18b). Regional effects controlled the development of internal structures such as asymmetric conjugate shear zones. Shear zones emphasize the interference between intrusion and regional deformation. They initiated during pluton cooling (Lagarde 1987), but they show geometric and kinematic compatibilities with the regional NW–SE shortening. Moreover, their asymmetric pattern is consistent with the sinistral wrenching described in adjacent country rocks.

Where prominent intrusive effects can be detected, the geometry and the kinematics of internal deformation are mainly controlled by the shape and the motion of the rising pluton (Figs. 18c–e). Within the Oulmes pluton intrusive effects led to high-temperature orthogneisses and normal shears concentrated in the outer parts of the pluton. Nevertheless the lack of microstructures registering medium- to low-temperature internal deformation history indicates that intrusive effects quickly abated. Within the lower parts of the Tichka pluton, concentric and inward-dipping orthogneisses, down-dip stretching lineations, and reverse senses of shear indicate upward rising of the magma. Within the Zaer monzogranite, peripheral flat lying orthogneisses with concentric patterns and predominant southward shears are consistent with the southwards spreading of a flat pluton.

These intrusive effects progressively decrease in country rocks surrounding plutons (Fig. 18). In the Oulmes aureole, the helicitic pattern of the flattening plane combined with shear criteria attest to regional sinistral wrenching during pluton emplacement (Ait Omar 1986, Diot *et al.* 1987). In the Tichka pluton, upward movement evolved to dextral wrenching along the Tizi n'Test Fault (Petit 1976, Lagarde & Roddaz 1983). In the Zaer aureole, southwards shearing evolved to dextral thrust-wrenching.

CONCLUSION

During the late Carboniferous, the Western Moroccan Hercynian belt experienced a phase of regional shortening leading to weak and low-grade deformation. This regional deformation is concentrated in zones of crustal weakness such as Proterozoic faults and thermally softened aureoles around late Carboniferous plutons.

Late Carboniferous granitic plutons of Morocco show various indicators of syntectonic emplacement at shallow crustal levels (Fig. 19).

(1) Plutons are distributed along lines parallel to reactivated pre-existing faults and ductile deformation is mainly located in the thermally softened area surrounding plutons. These two features suggest that deep Proterozoic faults focused melts at depth and localized both plutons and regional deformation within higher crustal levels.

(2) Plutons have in general elliptical shapes which are consistently oriented with respect to the regional strain field. Pluton shape (ellipticity), orientation and age can be correlated with strain history.

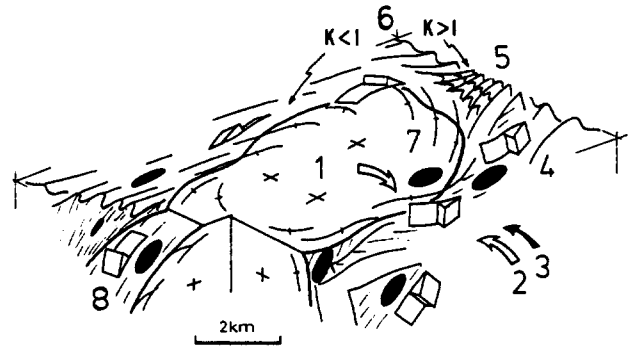

Fig. 19. Indicators of pluton emplacement during a regional deformation. 1: Elliptical shape oriented with respect to the regional strain field. 2: Finite strain gradients. 3: Increase of syntectonic contact metamorphism. 4: Perturbations of finite strain trajectories. 5: Schistosity triple points. 6: Changes in shape of the finite strain ellipsoid. 7: Foliation development in granitoids recording the decrease in temperature during pluton cooling. 8: Normal (or reverse) senses of shear indicating that country rock deformation and internal foliation development are contemporaneous with pluton final emplacement.

(3) A syntectonic low-pressure–high-temperature contact metamorphism is observed in the aureoles. Metamorphic assemblages indicate temperature increased towards plutons. Post-tectonic crystallization is related to thermal relaxation after intrusion.

(4) The microstructural evolution around syntectonic plutons is characterized by the tightening of folds in aureole rocks and by the progressive development of superimposed small-scale structures related to a progressive deformation.

(5) Perturbations of the strain field are related to pluton emplacement. Deformation is strongly heterogeneous. Finite strain gradients are detected within both country rocks and plutonic rocks. The increase in finite strain towards plutons accompanies development of superimposed structures. Highest strain intensities occur where shear zones bound plutons. Finite strain trajectories exhibit perturbations of the regional strain field around plutons (rotation of the regional flattening plane, development of structures conformable or slightly oblique to pluton boundaries, schistosity triple points). Internal structures, aureole structures and regional structures are contemporaneous and continuous. The strain ellipsoid evolved from dominant flattening types inside and outside plutons, to prolate types in the schistosity triple points. Plane strain evolving to prolate strain ellipsoids occurred in shear zones.

(6) Foliation development in granitoids shows a continuum between high-temperature and low-temperature solid-state foliations, related to the decrease of temperature during the thermal re-equilibration between pluton and country rocks.

These data point out the contribution of syn-tectonic plutons in understanding the record of geometry, intensity and kinematics of deformation. The geometry of the regional strain field is indicated by pluton orientations, and related strain trajectories. It is characterized, in the Western Morocco Hercynian belt, by a NW–SE shorten-

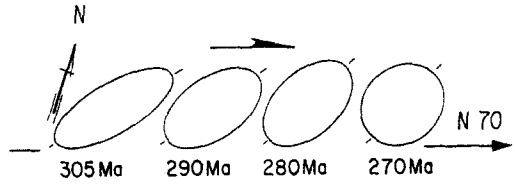

Fig. 20. Progressive deformation of the Western Moroccan Hercynian belt registered by late Carboniferous plutons. Each pluton records a short increment of the regional strain. Therefore the evolution with time of pluton ellipticity and orientation reflects the evolution of the incremental strain ellipse and indicates a decreasing ENE dextral shear strain.

ing direction (λ_3) and by an horizontal NE–SW stretching direction (λ_1).

Variations in strain intensity are indicated by pluton shapes (evolution with time of the ellipticity ratio) and by the obliquity of pluton long axes with respect to the regional shear plane. Syn-cooling deformation of plutons only records short increments of the regional strain (short-lived pluton cooling $<10^5$ years, Spera 1980). The evolution of pluton ellipticity and orientation will thus reflect the evolution of the incremental strain ellipse. In Western Morocco this evolution indicates a progressive decrease in strain intensity (decrease of ellipticity ratio and increase of pluton obliquity) (Fig. 20), suggesting that the Hercynian non-coaxial strain decreased between 320 and 280 Ma, and then vanished during the late tectonic emplacement of discordant alkaline granites.

Plutons can tell us a great deal about kinematic history. In Western Morocco they record extensive strike-slip motion which can be related to crustal-scale ENE dextral wrenching between Africa and Western Europe.

Acknowledgements—The authors wish to thank N. Ait Ayad, A. Chemsseddoha and A. Saquaque, from the Marrakech University, for their contribution to the knowledge of Moroccan plutons. Thanks are due to P. Choukroune, D. Gapais, J.-P. Brun, R. Capdevila and C. Le Corre for helpful discussions on granites. We are greatly indebted to D. Gapais, L. Harris, D. H. V. Hutton, C. Simpson and two anonymous referees for their constructive criticism.

REFERENCES

Ait Ayad, N. 1987. Modalités de mise en place du granite hercynien d'Azegour (Haute-Atlas Occidental, Maroc). Unpublished thèse 3ème cycle, University of Marrakech.

Ait Omar, S. 1986. Modalités de mise en place d'un pluton granitique et ses relations avec la déformation régionale: l'exemple du granite hercynien d'Oulmès (Maroc Central). Unpublished thèse, University of Rennes I.

Bateman, R. 1985. Aureole deformation by flattening around a diapir during *in situ* ballooning. The Cannibal creek granite. *J. Geol.* **93**, 293–310.

Bernardin, C. 1988. Interpretation gravimétrique et structure profonde de la meseta marocaine et de sa marge atlantique. Unpublished thése, University of Marseille.

Berthé, D. & Brun, J. P. 1980. Evolution of folds during progressive shear in the south Armorican shear zone, France. *J. Struct. Geol.* **2**, 127–133.

Berthé, D., Choukroune, P. & Jegouzo, P. 1979. orthogneiss, mylonite and non-coaxial deformation of granite: the example of the South Armorican Shear Zone. *J. Struct. Geol.* **1**, 31–42.

Blumenfeld, P. & Bouchez, J. L. 1988. Shear criteria in granite and migmatite deformed in the magmatic and solid state. *J. Struct. Geol.* **10**, 361–372.

Bonin, B. 1982. Les granites des complexes annulaires. *Manuels et Méthodes, Vol.* 4, B.R.G.M., France.

Brun, J.-P. & Cobbold, P. R. 1980. Strain heating in continental shear zones: a review. *J. Struct. Geol.* **2**, 149–158.

Brun, J.-P. & Pons, J. 1981. Strain patterns of pluton emplacement in a crust undergoing non-coaxial deformation, Sierra morena, Southern Spain. *J. Struct. Geol.* **3**, 219–229.

Burg, J.-P. 1987. Regional shear variation in relation to diapirism and folding. *J. Struct. Geol.* **9**, 925–934.

Burg, J.-P., Brunel, M., Gapais, D., Chen, G. M. & Liu, G. H. 1984. Deformation of leucogranites of the crystalline Main Central sheet in southern Tibet (China). *J. Struct. Geol.* **5**, 535–542.

Bussel, M. A. & Pitcher, W. S. 1985. The structural control of batholith emplacement. In: *Magnetism at Plate Edges; The Peruvian Andes*. Blackie, Glasgow, 167–176.

Cann, J. R. 1970. Upward movement of granite magma. *Geol. Mag.* **107**, 335–340.

Chemsseddoha, A. 1986. Cisaillement ductile et granites syntectoniques dans les Jebilet Centrales: l'exemple du pluton hercynien des Oulad-Ouaslam (Maroc). Unpublished thése 3ème cycle, University of Rennes.

Choubert, G. 1963. Histoire géologique du precambrien de L'Anti-Atlas. *Notes Mem. Serv. géol. Maroc.* **162**, 352.

Choukroune, P., Gapais, D. & Merle, O. 1987. Shear criteria and structural symmetry. *J. Struct. Geol.* **9**, 525–530.

Courrioux, G. 1987. Oblique diapirism: the Criffel granodiorite/granite zoned pluton (southwest Scotland). *J. Struct. Geol.* **3**, 313–330.

Cruden, A. R. 1988. Deformation around a rising diapir modeled by creeping flow past a sphere. *Tectonics* **5**, 1091–1101.

Diot, H. 1989. Mise en place des granitoides hercyniens de la meseta marocaine. Unpublished thèse d'état, University of Toulouse.

Diot, H., Bouchez, J.-L., Boutaleb, M. & Macaudiere, J. 1987. Le granite d'Oulmes. Maroc central. Structures de l'état magmatique à l'état solide et modèle de mise en place. *Bull. Soc. géol. Fr., III* **1**, 157–168.

Dunnet, D. 1969. A technique of finite strain analysis using elliptical particles. *Tectonophysics* **7**, 117–136.

Evans, J. P. 1988. Deformation mechanisms in granitic rocks at shallow crustal levels. *J. Struct. Geol.* **10**, 437–444.

Flinn, D. 1962. On folding during three-dimensional progressive deformation. *Q. Jl geol. soc. Lond.* **118**, 385–433.

Fry, N. 1979. Random points distributions and strain measurements in rocks. *Tectonophysics* **60**, 89–105.

Gapais, D. 1987. Les orthogneiss. Structures, mécanismes de déformation et analyse cinématique. Unpublished thèse d'Etat, University of Rennes.

Gapais, D. & Barbarin, B. 1986. Quartz fabric transition in a cooling syntectonic granite (Hermitage massif, France). *Tectonophysics* **125**, 357–370.

Gasquet, D., Leterrier, J., Mrini, Z. & Vidal, P. 1988. Caractérisation isotopique du massif du Tichkla (Haut Atlas, Maroc). *R.S.T., Lille*, 61.

Giuliani, G. & Sonet, J. 1982. Contribution à l'étude géochronologique du massif granitique hercynien des Zaer (Massif central marocain). *C. r. Acad. Sci., Paris* **294**, 139–143.

Hanmer, S. K. & Vigneresse, J. L. 1983. Le mécanisme de la mise en place de diapirs syntectoniques dans la chaîne hercynienne. Exemple des massifs leucogranitiques de Locronan et de Pontivy (Bretagne Centrale). *Bull. Soc. géol. Fr., XXII* **2**, 193–202.

Huon, S. 1965. Clivage ardoisier et réhomogenéisation isotopique K-Ar dans les schistes paléozoiques du Maroc. Unpublished thèse, University of Strasbourg.

Hutton, D. H. W. 1982. A tectonic model for the emplacement of the main Donegal Granite, N.W. Ireland. *J. geol. Soc. Lond.* **139**, 625–631.

Hutton, D. H. W. 1988. Granite emplacement mechanisms and tectonic controls: inferences from deformation studies. *Trans. R. Soc. Edinb., Earth Sci.* **79**, 245–255.

Lagarde, J. L. 1985. Cisaillements ductiles et plutons granitiques contemporains de la déformation hercynienne de la méseta marocaine. *Hercynica* **1**, 29–37.

Lagarde, J. L. 1987. Les plutons granitiques hercyniens marqueurs de la déformation crustale. Unpublished thèse d'Etat, University of Rennes.

Lagarde, J. L., Ait Ayad, N., Ait Omar, S., Chemsseddoha, A. & Saquaque, A. 1989. Plutons granitiqes tardi carbonifères marqueurs de la déformation crustale. L'exemple de la méseta marocaine. *C. r. Acad. Sci., Paris* **309**, 291–296.

Lagarde, J. L. & Choukroune, P. 1982. Cisaillement ductile et granitoïdes syntectoniques: l'exemple du massif hercynien des Jebilet (Maroc). *Bull. Soc. géol. Fr., XXIV* **2**, 299–307.

Lagarde, J. L. & Michard, A. 1986. Stretching normal to the regional thrust displacement in a thrust-wrench shear zone, Rehamna massif, Morocco. *J. Struct. Geol.* **8**, 483–492.

Lagarde, J. L. & Roddaz, B. 1983. Le massif plutonique du Tichka

(Haut Atlas, Maroc): un diapir syntectonique. *Bull. Soc. géol. Fr., XXV* **3**, 389–395.
Le Corre, C. 1978. Approche quantitative des processus synchisteux. L'exemple de segment hercynien de Bretagne Centrale. Unpublished thèse d'Etat, University of Rennes.
Le Corre, C. & Saquaque, A. 1987. Comportement d'un système pluton-encaissant dans un champ de déformation régional: le granite du Bramram (Jebilet, Maroc hercynien). *Bull. Soc. géol. Fr., III* **4**, 665–673.
Leymarie, P. 1968. Une méthode permettant de mettre en évidence le caractère ordonné de la distribution de gites mineraux. *Mineral. Deposita* **3**, 334–343.
Lister, G. S. & Williams, P. F. 1979. Fabric development in shear zones: theoretical controls and observed phenomena. *J. Struct. Geol.* **1**, 283–297.
Mabkhout, F., Bonin, B., Ait Ayad, N., Sirna, C. & Lagarde, J. L. 1988. Les massifs granitiques alcalins du permien marocain. *C. r. Acad. Sci., Paris* **307**, 162–168.
Mahmood, A. 1985. Emplacement of the zoned Zaer pluton, Morocco. *Bull. geol. Soc. Am.* **96**, 931–935.
Mahmood, A. & Bennani, A. 1984. S-type characteristics of the hercynian granitoïdes of the Central Palaeozoïc Massif, Morocco. *Geol. Mag.* **121**, 301–309.
Mattauer, M., Proust, F. & Tapponier, P. 1972. Major strike-slip fault of late hercynian age in Morocco. *Nature* **237**, 160–162.
Matte, P. 1986. La chaîne varisque parmi les chaînes paléozoiques péri atlantiques, modèle d'évolution et position des grands blocs continentaux au permo-carbonifère. *Bull. Soc. géol. Fr., VIII* **1**, 9–24.
Meneilly, A. W. 1982. Regional structure and syntectonic granite intrusion in the Dalradian of the Gweebarra Bay area, Donegal. *J. geol. Soc. Lond.* **139**, 633–646.
Mrini, Z. 1985. Age et origine des granitoides hercyniens du Maroc: apport de la géochronologie et de la géochimie isotopique. Unpublished thèse, University of Clermont.
Paterson, S. R. & Tobisch, O. T. 1988. Using pluton age to date regional deformation: problems with commonly used criteria. *Geology* **16**, 1108–1111.
Paterson, S. R., Vernon, R. H. & Tobisch, O. T. 1989. A review of the criteria for the identification of magmatic and tectonic foliations in granitoids. *J. Struct. Geol.* **11**, 349–363.
Petit, J. P. 1976. La zone de dècrochement du Tizi n'Test et son fonctionnement depuis le carbonifère (Maroc). Unpublished thèse 3eme cycle, University of Montpellier.
Piqué, A. 1982. Relations between stages of diagenetic and metamorphic evolution and the development of a primary cleavage in the north western Moroccan Meseta. *J. Struct. Geol.* **4**, 491–500.
Piqué, A. & Michard, A. 1989. Moroccan Hercynides: a synopsis. The Paleozoic evolution at the Northern margin of West Africa. *Am. J. Sci.* **289**, 286–330.
Pitcher, W. S. 1979. The nature, ascent and emplacement of granitic magmas. *J. geol. soc. Lond.* **136**, 627–662.
Pitcher, W. S. & Berger, A. R. 1972. *The Geology of Donegal: A Study of Granite Emplacement and Unroofing*. John Wiley, London.
Platt, J. P. & Vissers, R. L. M. 1980. Extensional structures in anisotropic rocks. *J. Struct. Geol.* **2**, 397–410.
Poirier, J. P. & Nicolas, A. 1975. Deformation—induced recrystallization due to progressive misorientation of subgrains with special reference to mantle peridotites. *J. Geol.* **83**, 707–720.
Ramberg, H. 1970. Model studies in relation to intrusion of plutonic bodies. In: *Mechanism of Igneous Intrusion. Geol. J.* **2**, 261–286.
Ramberg, H. 1981. *Gravity, Deformation and the Earth's Crust*. Academic Press, London.
Ramsay, J. G. 1967. *Folding and Fracturing of Rocks*. McGraw-Hill, New York.
Rosé, F. 1987. Les types granitiques du maroc hercynien. Unpublished thèse, University of Paris VI.
Sanderson, D. J. & Meneilly, A. W. 1981. Analysis of three-dimensional strain modified uniform distribution: andalusite fabrics from a granite aureole. *J. Struct. Geol.* **3**, 109–116.
Sibson, R. H. 1977. Fault rocks and fault mechanisms. *J. Geol. Soc.* **113**, 191–213.
Simpson, C. 1983. Strain and shape fabric variations associated with ductile shear zones. *J. Struct. Geol.* **5**, 61–72.
Simpson, C. & Schmid, S. M. 1983. An evaluation of criteria to deduce the sense of movement in sheared rocks. *Bull. geol. Soc. Am.* **94**, 1291–1298.
Soula, J. C. 1982. Characteristics and mode of emplacement of gneiss domes and plutonic domes in central-eastern Pyrenees. *J. Struct. Geol.* **4**, 313–342.
Spera, F. 1980. Thermal evolution of plutons: a parametrized approach. *Science* **207**, 299–301.
Talbot, C. J. 1974. Fold nappes as asymmetric mantled gneiss domes and ensialic orogeny. *Tectonophysics* **24**, 259–276.
Talbot, C. J. 1977. Inclined and asymmetric upward-moving gravity structures. *Tectonophysics* **42**, 159–181.
Termier, H., Agard, J. & Owodenko, B. 1950. Les gites d'étain et de tungstène de la région d'Oulmés (Maroc central). *Notes Mém. Serv. géol. Maroc* **82**, 326.
Termier, H. & Termier, G. 1971. Le massif granito-dioritique du Tichka (Haute-Atlas occidental, Maroc). *Notes Mém. Serv. géol. Maroc* **216**, 240.
Tisserant, D. 1977. Les isotopes du strontium et l'histoire hercynienne du Maroc, étude de quelques massifs atlasiques et mésetiens. Unpublished thèse 3eme cycle, University of Strasbourg.
Van den Bosch, J. W. H. 1974. Quelques principes généraux de l'interprétation gravimétrique illustrés par des exemples empruntés à la carte gravimétrique du Maroc. *Notes Mém. Serv. géol. Maroc* **255**, 117–136.
Vogel, T., Williams, E., Preston, J. & Walker, B. 1976. Origin of the Late Paleozoic plutonic Massifs in Morocco. *Bull. geol. Soc. Am.* **87**, 1753–1762.
Vigneresse, J. L. & Brun, J. P. 1983. Les leucogranites armoricains marqueurs de la déformation régionale: apport de la gravimétrie. *Bull. Soc. géol. Fr., XXV* **3**, 357–366.
Watterson, J. 1968. Homogeneous deformation of the gneisses of Vesterland, Southwest Greenland. *Bull. Grønl. geol. Unders.* **175**, 1–78.
White, S. H. & Knipe, R. J. 1978. On the geological significance of transformations and reaction enhanced ductility. *J. geol. soc. Lond.* **135**, 513–516.
Woidt, W. D. 1978. Finite elements calculations applied to salt dome analysis. *Tectonophysics* **50**, 369–386.

APPENDIX

The Hercynian granitoids from Western Morocco (petrographic types, Rb–Sr initial ratios, isotopic dating) from: (1) Tisserand (1977); (2) Mrini (1985); (3) Rosé (1987); (4) Gasquet *et al.* (1988)

Location	Petrographic types	Origin	Rb–Sr	Age (Ma)
1 Jebilet				
Central	I–S granodiorite	mixed	0.708	332 ± 5 (2)
	S monzogranite	crustal	0.712	306 ± 17 (2)
Eastern	I–S granodiorite	mixed		319 ± 10 (1)
2 Zaer	I–S granodiorite	mixed	0.705	303 ± 13 (2)
3 Oulmes	S monzogranite	crustal	0.710	298 ± 6 (2)
4 Tichka	I–S grandiorite	mixed		285 (4)
	Diorite, gabbro	mantle		
5 Zaer	S monzogranite	crustal	0.709	279 ± 11 (2)
6 W. Rehamna	Alkaline granitoids	mixed	0.705	268 ± 6 (2)
7 Ment	S monzogranite	crustal	0.715	270 ± 3 (2)
8 Azegour	Alkaline granitoids	mixed	0.705	271 ± 3 (2)